New Types of Blue, Red or Near IR Luminescent Phosphonate-Decorated Lanthanide Oxalates

Jun-Ling Song and Jiang-Gao Mao*[a]

Abstract: Hydrothermal reactions of the lanthanide chlorides with $MeN(CH_2CO_2H)(CH_2PO_3H_2)$, ($H_3L^1$) (or $Me_2NCH_2PO_3H_2$, H_2L^2) and sodium oxalate lead to seven new lanthanide oxalate phosphonate hybrids with three types of 3D network structures, namely, $[Ln(C_2O_4)\{MeNH(CH_2CO_2)(CH_2PO_3H)\}]\cdot 0.5H_2O$ (Ln = Nd: **1**; Eu: **2**; Gd: **3**), $[Ln_4(C_2O_4)_5(Me_2NHCH_2PO_3)_2(H_2O)_4]\cdot 2H_2O$ (Ln = La: **4**, Nd: **5**), $[Ln_3(C_2O_4)_4(Me_2NHCH_2PO_3)(H_2O)_6]\cdot 6H_2O$ (Gd: **6**, Er: **7**). Their structures have been established by X-ray single-crystal diffraction. Complexes **1**–**3** are isostructural and feature a 3D network formed by the interconnection of 3D network of $\{Ln(H_2L^1)\}^{2+}$ with 1D chains of $\{Ln(C_2O_4)\}^{+}$. Complexes **4** and **5** are isostructural and feature a complex 3D network built from 3D network of lanthanide oxalate and $\{Ln_4(HL^2)_2\}$ units. The isostructural **6** and **7** form another type of 3D network composed of porous lanthanide–oxalate network inserted by 1D chains of lanthanide–oxalate phosphonate. Compounds **1**, **5** and **7** are luminescent materials in the near IR region. Compounds **3** and **6** exhibit a broad blue fluorescent emission band at 451 and 467 nm, respectively. Compound **2** displays very strong and sharp emission bands at 592, 616 and 699 nm with a long luminescent lifetime of 1.13 ms.

Keywords: hydrothermal synthesis · inorganic–organic hybrids · lanthanides · luminescence

Introduction

The search for novel porous inorganic–organic hybrid materials based on metal phosphonates is of great research interest due to their potential applications in electro-optical, ion-exchange, catalysis and sensors.[1] The strategy of attaching functional groups such as crown ether, amine, hydroxyl, and carboxylate groups to the phosphonic acid has proven to be effective for the isolation of a variety of metal phosphonates with open-framework and microporous structures.[2–8] Most of the structural studies on metal phosphonates have been focused on the first row transition metals as well as main group metals such as Al^{III}, Ga^{III}, V^{V} or V^{IV} and Pb^{II}.[1–8] Reports on lanthanide phosphonates are rather limited and many of them are based on X-ray powder diffraction.[9–13] Lanthanide phosphonates normally have low solubility in water and other organic solvents, hence it is rendered difficult to obtain single crystals suitable for X-ray structural analysis. To improve the solubility and crystallinity of lanthanide phosphonates, additional function groups such as crown ether, carboxylate, hydroxyl and amine groups have been attached to the phosphonate ligand.[9–13] A series of lanthanide diphosphonates with a 3D pillared-layer structure were isolated by the Ferey group.[9] Several lanthanide phosphonates with a crown ether or calixarene moiety have been reported by Clearfield, Bligh, Lukes and Lin et al.[10] Their structures feature either a chelating mononuclear unit or a layer architecture.[10] A series of one dimensional lanthanide diphosphonates containing a hydroxyl group were reported.[11] A few 2D or 3D lanthanide phosphonates with additional carboxylate group or amino acid moiety were obtained.[12] Lanthanide compounds with phosphonic acid attached by Ph-, $PhCH_2$- or $NH_2CH_2CH_2$- group were obtained by the groups of Clearfield and Legendziewicz.[13] The elucidation of the structures of lanthanide phosphonates is very important since these compounds may exhibit useful luminescent properties in the visible and near IR region.[14] Results from our previous studies indicate that introducing a second ligand such as 5-sulfoisophthalic acid (H_3BTS); the lanthanide compounds of which have good solubility and very good crystallinity into the lanthanide–phosphonate system can lead to novel luminescent lanthanide–phosphonate hybrids with better solubility and crystallinity.[15] We

[a] J.-L. Song, Dr. J.-G. Mao
State Key Laboratory of Structure Chemistry
Fujian Institute of Research on the Structure of Matter
The Chinese Academy of Sciences, Fuzhou 350002 (P.R. China)
Fax: (+86) 591-837-14946
E-mail: mjg@ms.fjirsm.ac.cn

 DOI: 10.1002/chem.200400889

also hope that the combination of two types of ligands will enhance the energy-transfer efficiency from ligands to lanthanide ions and improve the luminescent properties of the lanthanide compounds due to the so-called "antenna effect".[14] Furthermore, the coordination of two types of ligands with the lanthanide ion may reduce or eliminate water molecules from the coordination sphere of the lanthanide(III) ion, hence increases the luminescent intensity and lifetime of the materials. As an expansion of our work on lanthanide phosphonates, we selected $MeN(CH_2CO_2H)(CH_2PO_3H_2)$, ($H_3L^1$) and $Me_2NCH_2PO_3H_2$, (H_2L^2) as the phosphonate ligands and oxalate as the second metal linker. Oxalic acid is a versatile ligand and has been reported to be able to form lanthanide and transition-metal complexes with various types of open framework and microporous structures.[16] Hydrothermal reactions of the above two types of ligands with lanthanide(III) chlorides afforded seven novel luminescent lanthanide(III) oxalate phosphonate hybrids with three types of 3D network structures, namely, $[Ln(C_2O_4)\{MeNH(CH_2CO_2)(CH_2PO_3H)\}]\cdot 0.5H_2O$ (Ln = Nd: **1**; Eu: **2**; Gd: **3**), $[Ln_4(C_2O_4)_5(Me_2NHCH_2PO_3)_2(H_2O)_4]\cdot 2H_2O$ (Ln = La: **4**, Nd: **5**), $[Ln_3(C_2O_4)_4(Me_2NHCH_2PO_3)(H_2O)_6]\cdot 6H_2O$ (Gd: **6**, Er: **7**). Herein we report their syntheses, crystal structures and luminescent properties.

Results and Discussion

Compounds **1**–**7** are the first members of lanthanide–oxalate phosphonates. They exhibit three different types of 3D network structures. Compounds **1**–**3** are isostructural, hence only the structure of **3** will be discussed in details as a representative. Different from layered lanthanide compounds containing both 5-sulfoisophthalate anion (BTS) and H_3L^1 ligands,[15] **3** features a 3D network structure. As shown in Figure 1, the gadolinium(III) ion is eight coordinated by four oxygen atoms from two oxalate anions, two carboxylate and two phosphonate oxygen atoms from four H_2L^1 anions. The Gd–O distances are in the range of 2.302(4) to 2.486(4) Å. Each oxalate anion is tetradentate and forms two Gd-O-C-C-O five-membered chelating rings. The H_2L^1 anion is tetradentate and bridges with four gadolinium(III) ions. One phosphonate oxygen atom is protonated, so does its amine group, which is due to the zwitterionic behavior of the aminophosphonic acid.[5]

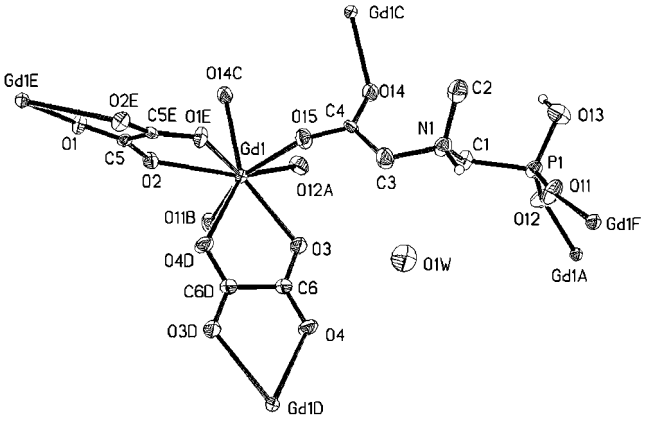

Figure 1. ORTEP representation of the selected unit in **3**. The thermal ellipsoids are drawn at 50% probability. Symmetry codes: A: $-x+1$, y, $-z+3/2$; B: $x-1/2$, $-y+1/2$, $z-1/2$; C: $-x+1$, $-y$, $-z+1$; D: $-x+1$, $-y+1$, $-z+1$; E: $-x+1$, y, $-z+1/2$; F: $x+1/2$, $-y+1/2$, $z+1/2$.

The interconnection of gadolinium(III) by chelating and bridging oxalate anions resulted in a 1D helix chain of $\{Gd(C_2O_4)\}^+$ (Figure 2a). The dihedral angle between two five-membered chelating rings sharing a common gadolinium(III) atom is 99.7°. The cross-linkage of gadolinium(III) ions by bridging H_2L^1 anions lead to a 3D network with tunnels along *b* axis (Figure 2b). The tunnel is formed by 16-mem-

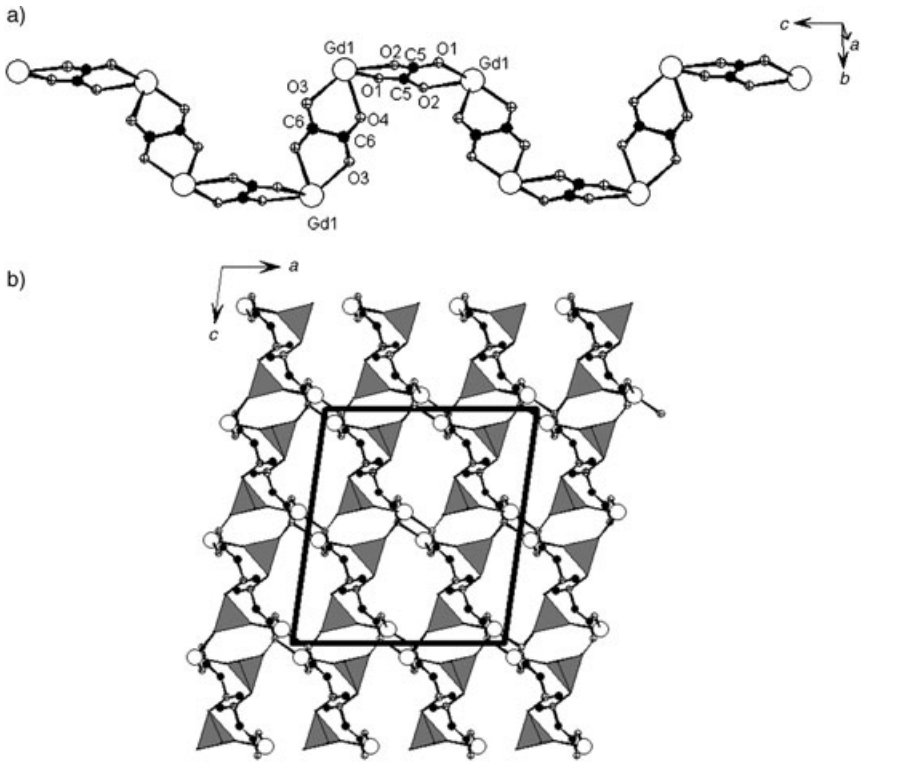

Figure 2. a) 1D helix chain of $\{Gd(C_2O_4)\}^+$ and b) 3D network of $\{Gd(H_2L^1)\}^{2+}$ in **3**. The phosphonate tetrahedra are shaded in gray. Gd, N, C, and O atoms are represented by open, octand, black and crossed circles, respectively.

bered rings composed of two gadolinium(III) ions and two H_2L^1 anions. Within the 3D network, each pair of gadolinium(III) ions are bridged by a pair of phosphonate groups, resulting in an eight-membered ring. The above-mentioned two building units are interconnected via sharing gadolinium(III) ions to form a complex 3D network (Figure 3). The structure of **3** can also be viewed as the oxalate anions occupying the tunnels of the 3D network of $\{Ln(H_2L^1)\}^{2+}$.

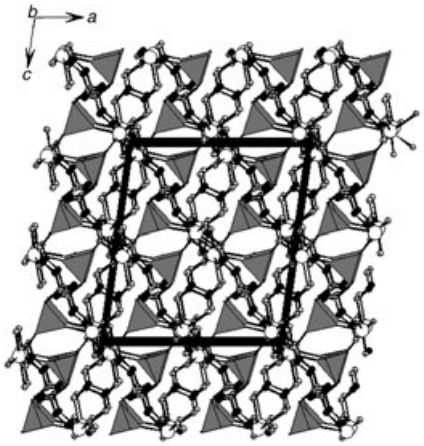

Figure 3. View of the structure of **3** down the *b* axis. The phosphonate tetrahedra are shaded in gray. Gd, N, C, and O atoms are represented by open, octand, black and crossed circles, respectively.

Complexes **4** and **5** are isostructural and only the structure of the neodymium(III) compound will be discussed in details as an example. There are two unique neodymium(III) ions in the asymmetric unit of **5**, as shown in Figure 4. Nd1 is eight-coordinated by six oxygen atoms from four oxalate anions, one phosphonate oxygen from one HL^2 anion and an aqua ligand, whereas Nd2 is nine-coordinated by five oxygen atoms from three oxalate anions, three phosphonate oxygens from two HL^2 anions as well as an aqua ligand. The Nd–O distances range from 2.348(5) to 2.537(5) Å, comparable to those reported for other neodymium(III) phosphonates and oxalates.[11–13,15,16] O2 (symmetry code $1-x$, $1-y$, $1-z$) is 2.960(6) Å away from Nd1, which is much longer than the remaining Nd–O distances. This bond, at the maximum, can be considered as the semi-chelation. The HL^2 anion is tetradentate, it chelates one neodymium(III) ion bidentately and also bridges with two other neodymium(III) ions. O12 is μ_2-bridging, whereas O11 and O13 are monodentate. There are two different coordination modes for the five oxalate anions in **5**. One oxalate anion is hexadentate. It forms two chelating rings with two lanthanide(III) ions and also bridges with two other lanthanide ions. The remaining four oxalate anions are tetradentate as that in **3**.

The interconnection of neodymium(III) atom by bridging and chelating HL^2 anions results in a $\{Nd_4(HL^2)_2\}$ unit, in which two Nd2 atoms are bridged by a pair of phosphonate groups to form a dimeric unit, and such dimeric unit further connects with two Nd2 atoms by μ^2-phosphonate oxygens

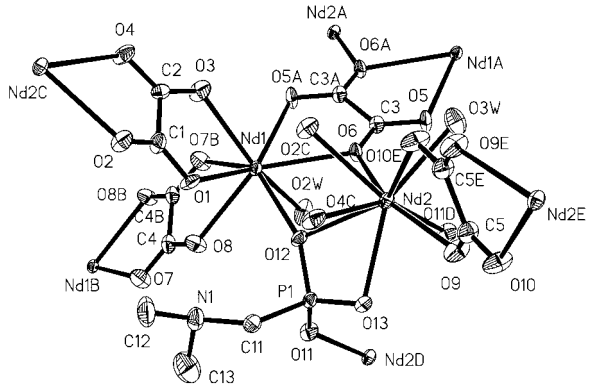

Figure 4. ORTEP representation of the selected unit in **5**. The lattice water molecules have been omitted for clarity. Thermal ellipsoids are drawn at 50% probability. Symmetry codes: A: $1-x$, $2-y$, $1-z$; B: $2-x$, $2-y$, $2-z$; C: $1-x$, $1-y$, $1-z$; D: $2-z$, $2-y$, $1-z$; E: $1-x$, $1-y$, $-z$.

(Figure 5a). The interconnection of the neodymium(III) ions by chelating and bridging oxalate anions lead to a 3D network of $\{Nd_4(C_2O_4)_5\}$ with tunnels running along *c* axis. The tunnel is formed by 24-membered rings composed of six neodymium(III) ions and six oxalate anions (Figure 5b). The above two types of building blocks are interconnected into a 3D network (Figure 6). The structure of **5** can also be viewed as the HL^2 anions being hung in the tunnels of $\{Nd_4(C_2O_4)_5\}$.

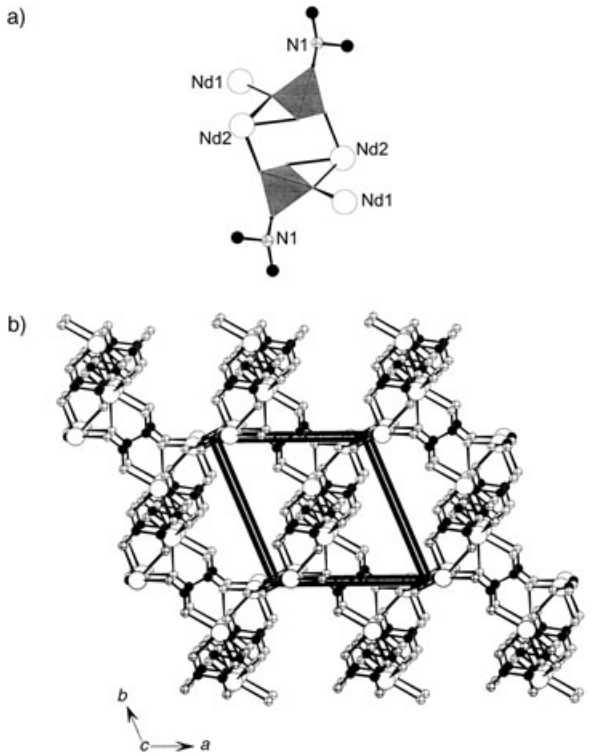

Figure 5. a) $\{Nd_4(HL^2)_2\}^{6+}$ unit and b) 3D network of $\{Nd_4(C_2O_4)_5\}^{2+}$ in **5**. The phosphonate tetrahedra are shaded in gray. Nd, N, C, and O atoms are represented by open, octand, black and crossed circles, respectively.

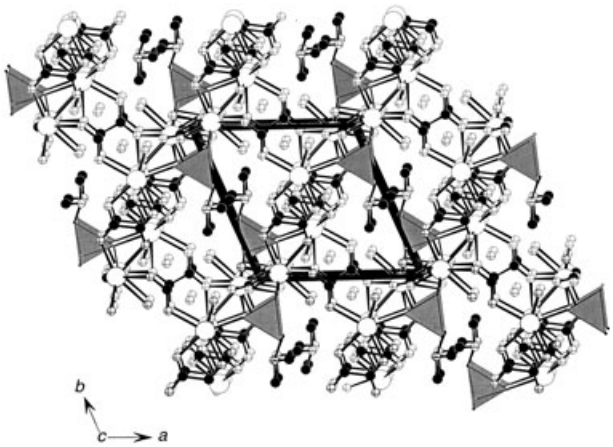

Figure 6. View of the structure of **5** down the *c* axis. The phosphonate tetrahedra are shaded in gray. Nd, N, C, and O atoms are represented by open, octand, black and crossed circles, respectively.

Complexes **6** and **7** are isostructural and form a 3D network different from that in compounds **4** and **5**. The structure of erbium(III) compound will be described in detail as an example. As shown in Figure 7, there are three unique erbium(III) ions in the asymmetric unit of **7**. Er1 is nine-coordinated by eight oxygen atoms from four oxalate anions and an aqua ligand. Er2 is eight-coordinated by six oxygen atoms from three oxalate anions, a phosphonate oxygen from one HL^2 anion and an aqua ligand. Er3 is eight-coordinated by two oxygen atoms from an oxalate anion, two phosphonate oxygen atoms from two HL^2 anions and four aqua ligands. The Er–O distances range from 2.180(6) to 2.444(6) Å, comparable to those reported for other erbium(III) phosphonates and oxalates.[11–13,16] The HL^2 anion is tridentate and bridges with three erbium(III) ions. All phosphonate oxygen atoms are unidentate, such coordination mode is different from the one in **4** and **5**. All oxalate anions in **6** and **7** adopt a same coordination mode as that in **3**.

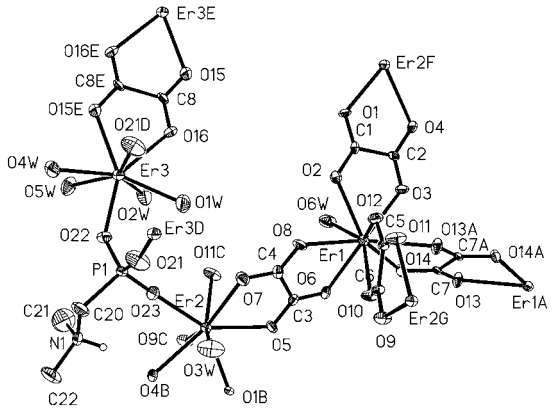

Figure 7. ORTEP representation of the selected unit in **7**. Thermal ellipsoids are drawn at 50% probability. The lattice water molecules have been omitted for clarity. Symmetry code: A: $-x$, $2-y$, $1-z$; B: $-1/2+x$, $3/2-y$, $1/2+z$; C: $1/2+x$, $3/2-y$, $1/2+z$; D: $-1-x$, $1-y$, $1-z$; E: $1/2+x$, $3/2-y$, $-1/2+z$; F: $-1/2+x$, $3/2-y$, $-1/2+z$; G: $-x$, $1-y$, $1-z$.

It is interesting to note that the interconnection of Er1 and Er2 atoms by three bridging and chelating oxalate anions lead to a porous 3D network of $\{Er_2(C_2O_4)_3\}$ (Figure 8a). Such network has not been reported in other erbium(III) oxalates. The large tunnel is formed by 40-membered rings composed of ten erbium(III) ions and ten oxalate anions. Each pair of Er3 atoms are bridged by two HL^2 anions to form a dimeric unit, such units are further interconnected by bridging and chelating oxalate anions into a 1D chain $\{Er(C_2O_4)(HL^2)\}$ along *a* axis (Figure 8b). It should be noted that the dimeric unit in $\{Er(C_2O_4)(HL^2)\}$ is different from that of $\{Nd_4(HL^2)_2\}$ in **5**, in that the phosphonate group in **5** forms an additional five-membered chelating ring with Nd2 atom. These 1D chains of lanthanide(III) oxalate phosphonate as well as the lattice water molecules are located at the large tunnels of $\{Er_2(C_2O_4)_3\}$ (Figure 9).

The IR spectra of **1**–**7** clearly exhibit the characteristic vibration bands for the phosphonate group (2760, 1230, 1110 cm^{-1}) and carboxylate groups (1630 and 1430 cm^{-1}). The broad bands at about 3420 cm^{-1} indicate the presence of water molecules in all compounds.

TGA curves for **1**–**3** are similar and exhibit two steps of weight losses. The Eu compound was used as an example (Figure 10). The weight loss before 350 °C corresponds to the release of the lattice water. The observed weight loss of 2.2% matches with the calculated value (2.1%). The second

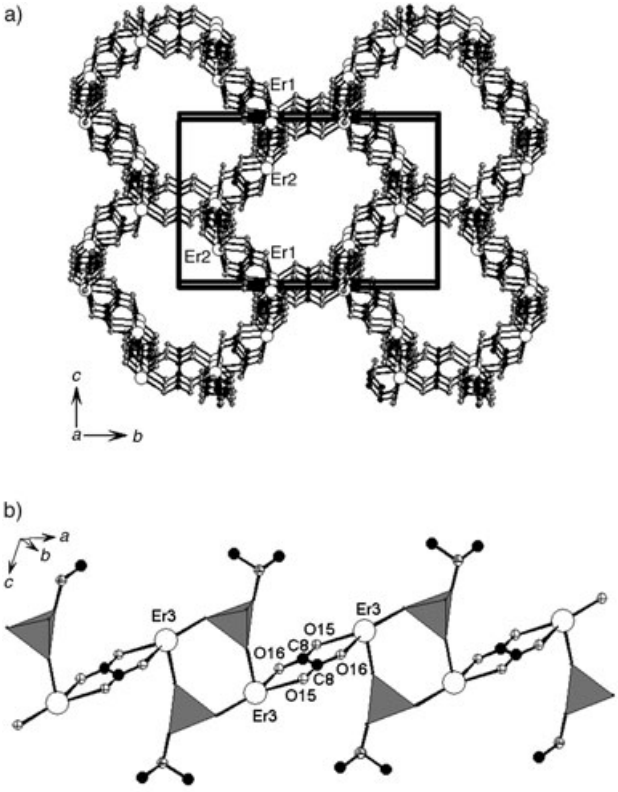

Figure 8. a) 3D porous network of $\{Er_2(C_2O_4)_3\}$ and b) 1D chain of $\{Er(C_2O_4)(HL^2)\}$ along *a* axis in **7**. The phosphonate tetrahedra are shaded in gray. Er, N, C, and O atoms are represented by open, octand, black and crossed circles, respectively.

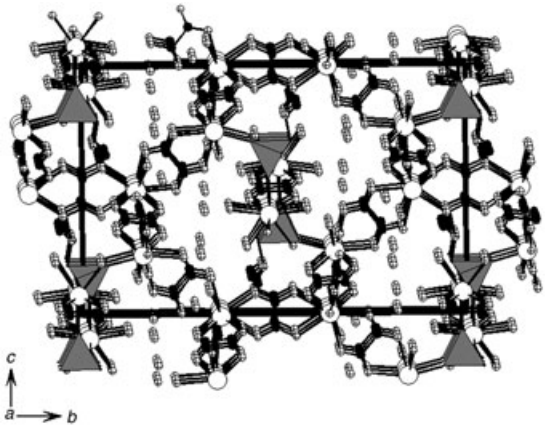

Figure 9. View of the crystal structure of **7** down the *a* axis. The phosphonate tetrahedra are shaded in gray. Er, N, C, and O atoms are represented by open, octand, black and crossed circles, respectively.

step began at 350 °C and was complete at 700 °C, during which the organic groups were burnt. The final residuals are $EuPO_4$. The observed total weight loss of 39.9 % is slightly smaller than the theoretical one (42.7 %). TGA diagrams of **4** and **5** are similar and reveal two main weight losses. **5** is used as an example (Figure 10). The first step corresponds to the loss of two lattice water molecules and four aqua ligands. The weight loss started at 66 °C and was completed at 215 °C. The observed weight loss of 7.4 % is close to the calculated value (7.7 %). The second step began at 232 °C and was complete at 661 °C, during which the organic groups were burnt. The final residuals are a mixture of two $NdPO_4$ and one Nd_2O_3. The observed total weight loss of 42.8 % is close to the theoretical one (41.9 %). TGA diagrams of **6** and **7** are similar and reveal two main weight losses. Complex **7** is used as an example (Figure 10). The first step started at 60 °C and was completed at 380 °C, corresponding to the release of six lattice water molecules and six aqua ligands. The observed weight loss of 18.2 % is close to the calculated value (17.9 %). The second step covering from 402 to 653 °C, corresponds to the combustion of the organic groups. The final residual is a mixture of one $ErPO_4$ and one Er_2O_3. The observed total weight loss of 44.2 % is slightly smaller than the calculated value (46.4 %).

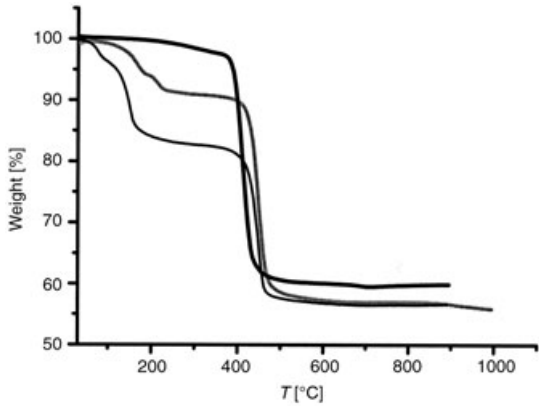

Figure 10. TGA curves for **2** (thick black), **5** (gray) and **7** (thin black).

Based on the XRD powder patterns, the frameworks of **1**–**7** can be retained after the release of lattice water molecules. These lattice waters can also be re-absorbed.

Luminescent properties: The solid-state luminescent properties of **1**–**7** were investigated at room temperature. Complex **4** shows no emission band under our experimental conditions. Sodium oxalate shows no emission in the visible region. The emission spectra of **1**–**3** and **5**–**7** are given in Figures 11–13. Under excitation of 826 nm, **1** and **5** display the characteristic emission bands for the neodymium(III) ion (Figure 11): a weak emission band at 883 nm (for **1**) or 896 nm for **5** ($^4F_{3/2} \rightarrow {}^4I_{9/2}$), strong emission bands at 1047

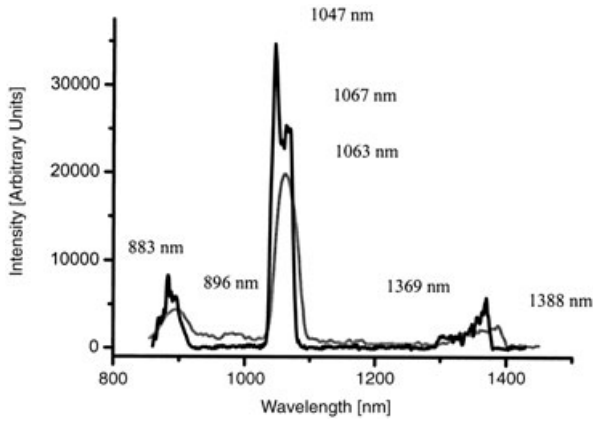

Figure 11. Solid-state emission spectra of **1** (black) and **5** (gray) at room temperature.

and 1067 nm for **1** or 1063 nm for **5** ($^4F_{3/2} \rightarrow {}^4I_{11/2}$) and a very weak band at 1369 nm for **1** or 1388 nm for **5** ($^4F_{3/2} \rightarrow {}^4I_{13/2}$) in the near IR region.[15,17] The Nd ($^4F_{3/2}$) lifetimes were measured to be 33.0 and 18.7 μs, respectively for **1** and **5**. The emission spectra of **3** and **6** only exhibit a broad blue fluorescent emission band at $\lambda_{max} = 451$ nm (ex = 370 nm) for **3** or $\lambda_{max} = 467$ nm (ex = 375 nm) for **6** (Figure 12), which corresponds to a ligand-centered (LC) fluorescence. The metal-centered (MC) electronic levels of Gd^{3+} ion are known to be located at 31 000 cm^{-1}, typically well above the ligand-centered electronic levels of organic ligands. Therefore, ligand-to metal energy transfer and the consequent MC luminescence cannot be observed.[18] Complex **2** exhibits three very strong characteristic emission bands for the europium(III) ion in the visible region under excitation at 394 nm (Figure 13a). These emission bands are 592 ($^5D_0 \rightarrow {}^7F_1$), 616 ($^5D_0 \rightarrow {}^7F_2$) and 699 nm ($^5D_0 \rightarrow {}^7F_4$). The Eu ($^5D_0$) lifetime of **2** for $\lambda_{ex,em} = 394$, 616 nm is 1.13 ms. The emission spectrum of **7** shows two comparable strong emission bands at 1545 and 1561 nm under 980 nm excitation (Figure 13b), both can be attributed to the $^4I_{13/2} \rightarrow {}^4I_{15/2}$ transition for the Er^{3+} ion.[17,18] The two close bands observed are probably due to the $^4I_{13/2} \rightarrow {}^4I_{15/2}$ transition band being split by three erbium(III) ions with different coordination geometries.

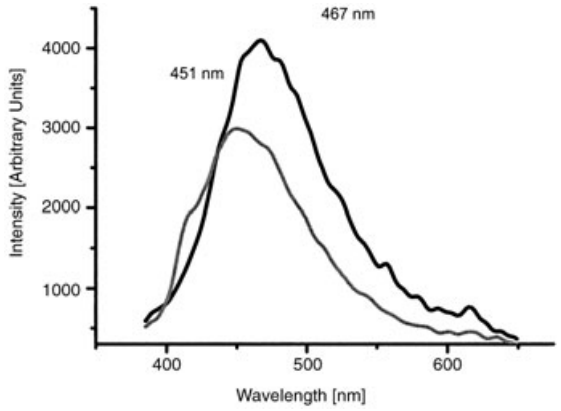

Figure 12. Solid-state emission spectra of **3** (gray) and **6** (black) at room temperature.

The luminescence spectra recorded after the release of lattice water molecules are similar to those for compounds with lattice water molecules, however, the intensities of the emission bands for these dehydrated species are significantly enhanced. The lower intensities of the emission bands for those hydrated compounds are due to the quenching effect of the luminescent state by high-frequency vibrating water molecules.[15] The enhancements in intensity for the dehydrated compounds of **5**–**7** are much greater than those of **1**–**3**, which is due to fewer lattice water present in **1**–**3**.

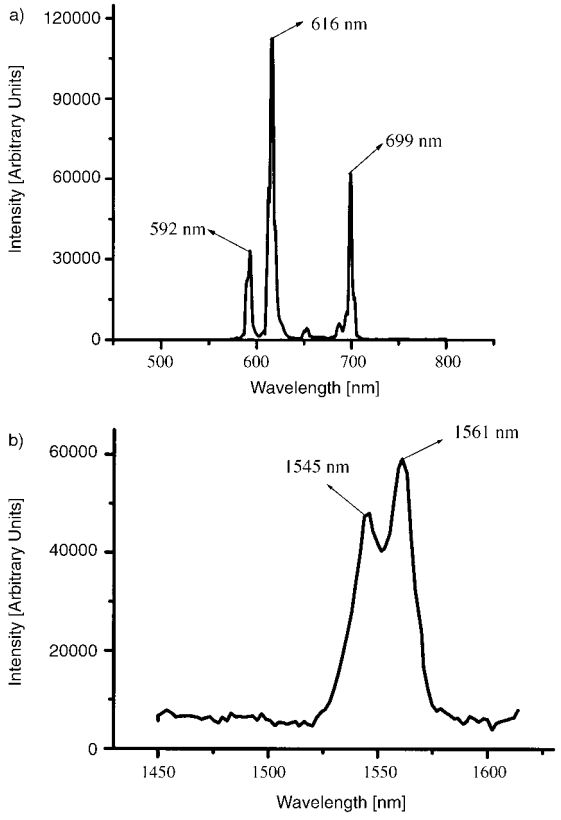

Figure 13. Solid-state emission spectra of a) **2** and b) **7** at room temperature.

These results indicate that **3** and **6** are capable of producing blue light in electro-luminescent devices, whereas **1**, **5** and **7** are luminescent materials in the near IR region. Compound **2** is a good candidate for red-light luminescent material.

Conclusion

In summary, the hydrothermal syntheses, crystal structures and luminescent properties of seven novel rare-earth oxalate phosphonates have been described. Their structures can be viewed as lanthanide phosphonate-based networks being decorated by oxalate ligands (for **1**–**3**) or lanthanide oxalate-based 3D networks being decorated by phosphonate ligands (for **4**–**7**). Complexes **1**–**3** and **5**–**7** are new examples of rare-earth materials with blue, red luminescent or near-infrared emission. Lanthanide compounds with a phosphonate ligand such as H_2L^2 normally have low solubility in water and poor crystallinity, we can greatly improve their solubility and crystallinity by introducing oxalic acid as the second metal linker. This synthetic technique also allows us to design new types of lanthanide complexes with novel crystal structures and physical properties. We believe that a wide range of new lanthanide open frameworks and microporous materials can be developed by self-assembly or structural directed synthesis using a similar technique.

Experimental Section

Materials and instrumentations: $MeN(CH_2CO_2H)(CH_2PO_3H_2)$, ($H_3L^1$) and $H_2O_3PCH_2N(CH_2CO_2H)_2$, ($H_4PMIDA$) and $Me_2NCH_2PO_3H_2$, (H_2L^2) were prepared by a Mannich-type reaction according to procedures described previously.[8a] All other chemicals were obtained from commercial sources and used without further purification. Elemental analyses were performed on a Vario EL III elemental analyzer. Thermogravimetric analyses were carried out on a NETZSCH STA 449C unit at a heating rate of 15 °C min^{-1} under a nitrogen atmosphere. IR spectra were recorded on a Magna 750 FT-IR spectrometer photometer as KBr pellets in the 4000–400 cm^{-1}. X-ray powder diffraction (XRD) patterns ($Cu_{K\alpha}$) were collected in a sealed glass capillary on a XPERT-MPD θ-2θ diffractometer. Photoluminescence analyses were performed on an Edinburgh FLS920 fluorescence spectrometer.

Preparation of [Ln(C_2O_4)(H_2L^1)]·0.5H_2O (Ln = Nd: 1, Eu: 2, Gd: 3): A mixture of $LnCl_3 \cdot 6H_2O$ (0.18 g, 0.5 mmol), H_3L^1 (0.10 g 0.5 mmol) and $Na_2C_2O_4$ (0.07 g, 0.5 mmol) in distilled water (10 mL) was sealed in an autoclave equipped with a Teflon liner (25 mL), and then heated at 165 °C for 4 d. Crystals of **1** (purple), **2**, and **3** were collected in about 38 % for **1**, 42 % for **2**, 45 % yield for **3** (based on the lanthanide). The initial and final pH values of the resultant solution were 2.5 and 3.0, respectively. Complex **1**: IR (KBr): $\tilde{\nu}$ = 3362(brm), 3019(w), 2955(w), 2760(w), 1607(m), 1615(vs), 1466(w), 1403(m), 1331(m), 1329(m), 1236(s), 1100(s), 1010(w), 960(w), 956(w), 909(s), 791(s), 711(m), 593(w), 519(m), 476 cm^{-1} (m); complex **2**: IR (KBr): $\tilde{\nu}$ = 3411(brm), 3020(w), 2956(w), 2761(w), 2346(w), 1751(w), 1693(m), 1618(vs), 1560(m), 1466(m), 1404(m), 1342(w), 1326(m), 1257(m), 1238(m), 1105(vs), 1011(w), 960(m), 934(w), 909(s), 792(s), 721(w), 711(w), 584(w), 528(w), 476(m); complex **3**: IR (KBr): $\tilde{\nu}$ = 3421(brm), 2978(w), 2651(w), 2346(w), 1630(m), 1638(vs), 1469(w), 1364(w), 1318(m), 1175(s), 1132(w), 1071(s), 1014(m), 982(w), 831(w), 798(m), 773(w), 671(w), 582(w), 494(w); elemental analysis calcd (%) for **1**: C 16.96, H 2.49, N 3.36;

Table 1. Crystal data and structure refinements for **2–7**.

	2	**3**	**4**
formula	$C_6H_{10}EuNO_{9.5}P$	$C_6H_{10}GdNO_{9.5}P$	$C_{16}H_{30}La_4N_2O_{32}P_2$
color	colorless	colorless	colorless
F_w	431.08	436.37	1380.00
space group	$C2/c$	$C2/c$	$P\bar{1}$
a [Å]	13.9723(5)	14.0040(5)	9.4258(9)
b [Å]	10.7349(4)	10.7125(4)	10.966(1)
c [Å]	15.6958(4)	15.6716(3)	11.049(1)
α [°]	90.0	90.0	117.290(2)
β [°]	98.147(2)	98.036(2)	91.203(2)
γ [°]	90.0	90.0	109.647(2)
V [Å^3]	2330.5(1)	2327.9(1)	934.6(2)
Z	8	8	2
ρ_{calcd} [g cm^{-3}]	2.457	2.490	2.452
μ [mm^{-1}]	5.566	5.881	4.676
GOF on F^2	1.239	1.197	1.149
$R1$, $wR2$ ($I>2\sigma(I)$)[a]	0.0483/0.0963	0.0295/0.0621	0.0329/0.0700
$R1$, $wR2$(all data)	0.0509/0.0987	0.0351/0.0662	0.0412/0.0761
	5	**6**	**7**
formula	$C_{16}H_{30}Nd_4N_2O_{32}P_2$	$C_{11}H_{33}Gd_3NO_{31}P$	$C_{11}H_{33}Er_3NO_{31}P$
color	purple	colorless	pink
F_w	1401.32	1178.10	1208.13
space group	$P\bar{1}$	$P2_1/n$	$P2_1/n$
a [Å]	9.3948(3)	10.2481(2)	10.0476(1)
b [Å]	10.7213(3)	22.3910(3)	22.2426(2)
c [Å]	10.8727(4)	15.0697(3)	14.9869(2)
α [°]	116.310(1)	90.0	90.0
β [°]	91.804(1)	108.02(1)	107.586(1)
γ [°]	109.869(1)	90.0	90.0
V [Å^3]	901.46(5)	3288.3(1)	3192.81(6)
Z	2	4	4
ρ_{calcd} [g cm^{-3}]	2.581	2.380	2.513
μ [mm^{-1}]	5.868	6.141	7.978
GOF on F^2	1.108	1.206	1.132
$R1$, $wR2$ ($I>2\sigma(I)$)[a]	0.0343/0.0901	0.0486/0.0963	0.0381/0.0767
$R1$, $wR2$(all data)	0.0386/0.0963	0.0597/0.1016	0.0488/0.0818

[a] $R1=\Sigma||F_o|-|F_c||/\Sigma|F_o|$, $wR2=\{\Sigma w[(F_o)^2-(F_c)^2]^2/\Sigma w[(F_o)^2]^2\}^{1/2}$.

found: C 17.02, H 2.38, N 3.31; for **2**: C 16.63, H 2.46, N 3.38; found: C 16.72, H 2.34, N 3.25; for **3**: C 16.46, H 2.43, N 3.26; found: C 16.51, H 2.31, N 3.21.

Preparation of $[Ln_4(C_2O_4)_5(HL^2)_2(H_2O)_4]\cdot 2H_2O$ (Ln = La: 4, Nd: 5) and $[Ln_3(C_2O_4)_4(HL^2)(H_2O)_6]\cdot 6H_2O$ (Gd: 6, Er: 7): Compounds **4–7** were initially synthesized by hydrothermal reaction of lanthanide chloride, H_4PMIDA and sodium oxalate at 165 °C in about 48, 45, 46 and 36% yield (based on lanthanide metal), respectively. Subsequent structural analyses indicate that the two carboxylate groups of H_4PMIDA had been cleaved to form a new phosphonate ligand, $Me_2NCH_2PO_3H_2$ (H_2L^2). Therefore **3–7** were re-synthesized by using $Me_2NCH_2PO_3H_2$ (H_2L^2) directly. $LnCl_3\cdot 6H_2O$ (0.5 mmol), $Me_2NCH_2PO_3H_2$ (0.5 mmol) and $Na_2C_2O_4$ (0.5 mmol) were dissolved in distilled water (10 mL). The pH value of the resultant solution was adjusted to about 4.5 by slow addition of NaOH. Then the mixture was sealed into an autoclave equipped with a Teflon liner (25 mL) and heated at 165 °C for 4 d. Crystals of **4–7** were collected in about 68, 59, 56 and 48% yield (based on lanthanide metal), respectively. The final pH values of the solutions were about 3.5. The purity of these compounds was also confirmed by X-ray powder patterns and elemental analyses. Complex **4**: IR (KBr): $\tilde{\nu}$ = 3422(br), 2756(w), 1634(vs), 1466(w), 1404(w), 1327(w), 1259(w), 1237(w), 1172(w), 1106(s),

Table 2. Selected bond lengths [Å] and angles [°] for **2–7**.

Ln–O	**2** (Eu)	**3** (Gd)	Ln–O	**4** (La)	**5** (Nd)	Ln–O	**4** (La)	**5** (Nd)
Ln1–O(12)#1	2.305(6)	2.302(4)	Ln1–O12	2.400(4)	2.348(5)	Ln2–O11#4	2.425(5)	2.373(5)
Ln1–O11#2	2.327(6)	2.314(4)	Ln1–O3	2.475(5)	2.412(5)	Ln2–O9	2.530(5)	2.466(6)
Ln1–O15	2.347(6)	2.334(4)	Ln1–O5#1	2.531(5)	2.484(5)	Ln2–O4#3	2.550(5)	2.493(5)
Ln1–O14#3	2.440(6)	2.427(4)	Ln1–O8	2.539(5)	2.481(6)	Ln2–O13	2.556(5)	2.522(5)
Ln1–O3	2.453(6)	2.439(4)	Ln1–O7#2	2.540(5)	2.492(6)	Ln2–O10#5	2.579(5)	2.548(6)
Ln1–O4#4	2.453(6)	2.434(4)	Ln1–O1	2.568(5)	2.503(5)	Ln2–O2#3	2.603(5)	2.526(5)
Ln1–O1#5	2.484(6)	2.475(4)	Ln1–O2W	2.579(5)	2.489(6)	Ln2–O6	2.609(4)	2.570(5)
Ln1–O2	2.498(5)	2.486(4)	Ln1–O6	2.582(4)	2.537(5)	Ln2–O3W	2.623(5)	2.540(6)
						Ln(2)–O(12)	2.642(4)	2.570(6)
Ln–O	**6** (Gd)	**7** (Er)	Ln-O	**6** (Gd)	**7** (Er)	Ln–O	**6** (Gd)	**7** (Er)
Ln1–O8	2.415(7)	2.376(6)	Ln2–O23	2.219(7)	2.188(6)	Ln3–O21#4	2.239(9)	2.180(7)
Ln1–O14	2.415(6)	2.359(6)	Ln2–O1#2	2.374(7)	2.330(5)	Ln3–O22	2.281(8)	2.243(6)
Ln1–O2	2.418(7)	2.389(6)	Ln2–O9#3	2.381(7)	2.346(6)	Ln3–O5W	2.427(7)	2.380(6)
Ln1–O10	2.421(7)	2.378(6)	Ln2–O7	2.391(6)	2.348(6)	Ln3–O2W	2.443(8)	2.400(7)
Ln1–O12	2.438(7)	2.382(6)	Ln2–O5	2.424(6)	2.379(6)	Ln3–O4W	2.456(8)	2.405(6)
Ln1–O6	2.446(6)	2.417(6)	Ln2–O11#3	2.431(7)	2.395(6)	Ln3–O1W	2.463(8)	2.404(7)
Ln1–O3	2.455(7)	2.415(6)	Ln2–O3W	2.435(9)	2.371(7)	Ln3–O15#5	2.463(7)	2.433(6)
Ln1–O6W	2.468(8)	2.407(6)	Ln2–O4#2	2.451(7)	2.412(6)	Ln3–O16	2.480(8)	2.444(6)
Ln1–O13#1	2.541(7)	2.526(6)						

Symmetry transformations used to generate equivalent atoms: For **2** and **3**: #1: $-x+1$, y, $-z+3/2$; #2: $x-1/2$, $-y+1/2$, $z-1/2$; #3: $-x+1$, $-y$, $-z+1$; #4: $-x+1$, $-y+1$, $-z+1$; #5: $-x+1$, y, $-z+1/2$; for **4** and **5**: #1: $-x+1$, $-y+2$, $-z+1$; #2: $-x+1$, $-y+1$, $-z$; #3: $-x+1$, $-y+1$, $-z+1$; #4: $-x+2$, $-y+2$, $-z+1$; #5: $-x+2$, $-y+2$, $-z+2$; for **6** and **7**: #1: $-x$, $-y+2$, $-z+1$; #2: $x+1/2$, $-y+3/2$, $z-1/2$; #3: $x-1/2$, $-y+3/2$, $z-1/2$; #4: $-x$, $-y+1$, $-z+1$; #5: $-x-1$, $-y+1$, $-z+1$.

1012(w), 909(m), 794(m), 711(w), 584(w), 522(w), 476 cm^{-1} (w)**;** complex **5**: IR (KBr): $\tilde{\nu}$ = 3430(br), 2742(w), 1633(vs), 1313(m), 1170(s), 1130(w), 1065(m), 1010(m), 977(w), 792(m), 578(w), 493(w); complex **6**: IR (KBr): $\tilde{\nu}$ = 3410(br), 2741(w), 1652(vs), 1622(vs), 1471(w), 1318(m), 1159(m), 1116(s), 1041(w), 806(m), 680(w), 578(w), 493(w); complex **7**: IR (KBr): $\tilde{\nu}$ = 3410(br), 2736(w), 1654(vs), 1625(vs), 1478(w), 1361(w), 1320(m), 1165(m), 1116(s), 1047(m), 974(w), 808(m), 682(w), 586(w), 485(w); elemental analysis calcd (%) for **4**: C 13.93, H 2.19, N 2.03; found: C 13.96, H 2.36, N 1.98; for **5**: C 13.71, H 2.16, N 2.00; found: C 13.78, H 2.34, N 1.96; for **6**: C 11.21, H 2.82, N 1.19; found: C 11.28, H 2.96, N 1.08; for **7**: C 10.94, H 2.75, N 1.16; found: C 10.98, H 2.96, N 1.09.

Single-crystal structure determination: Single crystals of **2–7** were mounted on a Siemens Smart CCD diffractometer equipped with a graphite-monochromated $Mo_{K\alpha}$ radiation (λ = 0.71073 Å). Intensity data were collected by the narrow frame method at 293 K. The data sets were corrected for Lorentz and Polarization factors as well as for empirical absorption based on ψ scan technique. Both structures were solved by the direct methods and refined by full-matrix least-squares fitting on F^2 by SHELX-97.[19] All non-hydrogen atoms were refined with anisotropic thermal parameters. Hydrogen atoms were located at geometrically calculated positions and refined with isotropic thermal parameters. Crystallographic data and structural refinements for **2–7** are summarized in Table 1. Important bond lengths for **2–7** are listed in Table 2. Compound **1** was isostructural with **2** and **3** based on its cell parameters (monoclinic C lattice with a = 14.0424(14), b = 10.8676(11), c = 15.8029(16) Å, β = 98.196(2)°, V = 2387.0(4) $Å^3$), and no data collection was performed.

CCDC-248786–248791 (**2–7**) contain the supplementary crystallographic data for this paper. These data can be obtained free of charge from The Cambridge Crystallographic Data Centre via www.ccdc.cam.ac.uk/data_request/cif

Acknowledgements

This work was supported by the National Natural Science Foundation of China (20371047), NSF of Fujian Province (No. E0420003).

[1] a) A. Clearfield, Metal phosphonate chemistry in *Progress in Inorganic Chemistry, Vol. 47* (Ed.: K. D. Karlin), Wiley, New York, **1998**, pp. 371–511 (and references therein); b) A. Clearfield, in *New Developments in Ion Exchange Materials* (Eds.: M. Abe, T. Kataoka, T. Suzuki), Kodansha, Tokyo, **1991**.

[2] a) A. K. Cheetham, G. Ferey, T. Loiseau, *Angew. Chem.* **1999**, *111*, 3466–3492; *Angew. Chem. Int. Ed.* **1999**, *38*, 3268–3292; b) J. Zhu, X. Bu, P. Feng, G. D. Stucky, *J. Am. Chem. Soc.* **2000**, *122*, 11563–11564; c) M. Riou-Cavellec, M. Sanselme, N. Guillou, G. Ferey, *Inorg. Chem.* **2001**, *40*, 723–725; d) K. Barthelet, D. Riou, G. Ferey, *Solid State Sci.* **2001**, *3*, 203–209; e) D. Riou, C. Serre, J. Provost, G. Ferey, *J. Solid State Chem.* **2000**, *155*, 238–242; f) M. Riou-Cavellec, M. Sanselme, G. Ferey, *J. Mater. Chem.* **2000**, *10*, 745–748.

[3] a) F. Fredoueil, M. Evain, D. Massiot, M. Bujoli-Doeuff, P. Janvier, A. Clearfield, B. Bujoli, *J. Chem. Soc. Dalton Trans.* **2002**, 1508–1512; b) P. Rabu, P. Janvier, B. Bujoli, *J. Mater. Chem.* **1999**, *9*, 1323–1326; c) S. Drumel, P. Janiver, P. Barboux, M. Bujoli-Doeuff, B. Bujoli, *Inorg. Chem.* **1995**, *34*, 148–156.

[4] a) N. Stock, S. A. Frey, G. D. Stucky, A. K. Cheetham, *J. Chem. Soc. Dalton Trans.* **2000**, 4292–4296; b) S. Ayyappan, G. D. Delgado, A. K. Cheetham, G. Ferey, C. N. R. Rao, *J. Chem. Soc. Dalton Trans.* **1999**, 2905; c) A. Distler, S. C. Sevov, *Chem. Commun.* **1998**, 959–960; d) S. J. Hartman, E. Todorov, C. Cruz, and S. C. Sevov, *Chem. Commun.* **2000**, 1213–1214.

[5] a) D. Kong, Y. Li, J. H. Ross Jr, A. Clearfield, *Chem. Commun.* **2003**, 1720–1721; b) D. Kong, L. Yang, O. Xiang, A. V. Prosvirin, H. Zhao, J. H. Ross, Jr., K. M. Dunbar, A. Clearfield, *Chem. Mater.* **2004**, *16*, 3020–3031; c) J.-G. Mao, Z. Wang, A. Clearfield, *J. Chem. Soc. Dalton Trans.* **2002**, 4541–4546; d) J.-G. Mao, Z. Wang, A. Clearfield, *Inorg. Chem.* **2002**, *41*, 3713–3720; e) J.-G. Mao, Z. Wang, A. Clearfield, *New J. Chem.* **2002**, *26*, 1010–1014.

[6] a) P. Yin, L.-M. Zheng, S. Gao, X.-Q. Xin, *Chem. Commun.* **2001**, 2346–2347; b) L.-M. Zheng, S. Gao, H.-H. Song, S. Decurtins, A.-J. Jacobson, X.-Q. Xin, *Chem. Mater.* **2002**, *14*, 3143–3147; c) L.-M. Zheng, P. Yin, X.-Q. Xin, *Inorg. Chem.* **2002**, *41*, 4084–4086.

[7] a) E. Burkholder, V. Golub, C. J. O'Connor, J. Zubieta, *Chem. Commun.* **2003**, 2128–2129; b) R. C. Finn, E. Burkholder, J. Zubieta, *Chem. Commun.* **2001**, 1852–1853; c) R. C. Finn, J. Zubieta, *Inorg. Chem.* **2001**, *40*, 2466–2467; d) R. C. Finn, E. Burkholder, J. Zubieta, *Inorg. Chem.* **2001**, *40*, 3745–3754.

[8] a) C. Lei, J.-G. Mao, Y.-Q. Sun, H.-Y. Zeng, A. Clearfield, *Inorg. Chem.* **2003**, *42*, 6157–6159; b) J.-L. Song, J.-G. Mao, Y.-Q. Sun, A. Clearfield, *Eur. J. Inorg. Chem.* **2003**, 4218–4226; c) S.-M. Ying, J.-G. Mao, *Eur. J. Inorg. Chem.* **2004**, 1270–1276; d) J.-L. Song, C. Lei, Y.-Q. Sun, J.-G. Mao, *J. Solid State Chem.* **2004**, *177*, 2556–2563.

[9] a) F. Serpaggi, G. Ferey, *Inorg. Chem.* **1999**, *38*, 4741–4744; b) F. Serpaggi, G. Ferey, *J. Mater. Chem.*, **1998**, *8*, 2749–2755.

[10] a) O. R. Evans, H. L. Ngo, W.-B. Lin, *J. Am. Chem. Soc.* **2001**, *123*, 10395–10396; b) H. L. Ngo, W.-B. Lin, *J. Am. Chem. Soc.* **2002**, *124*, 14298–14299; c) A. Clearfield, C. V. K. Sharma, B.-L. Zhang, *Chem. Mater.* **2001**, *13*, 3099–3112; d) S. W. A. Bligh, N. Choi, C. F. G. C. Geraldes, S. Knoke, M. McPartlin, M. J. Sanganee, T. M. Woodroffe, *J. Chem. Soc. Dalton Trans.* **1997**, 4119–4125; e) J. Plutnar, J. Rohovec, J. Kotek, Z. Zak, I. Lukes, *Inorg. Chim. Acta* **2002**, *335*, 27–35.

[11] a) K. L. Nash, R. D. Rogers, J. Ferraro, J. Zhang, *Inorg. Chim. Acta* **1998**, *269*, 211–223; b) L. V. Meervelt, P. Martello, J. P. Silvestre, R. Rochdaoui, M. R. Lee, N. Q. Dao, C. G. Walrand, *Z. Kristallogr.* **2002**, *217*, 27–34; c) J. P. Silvestre, N. Q. Dao, M. R. Lee, *Phosphorus Sulfur* **2001**, *176*, 173–183; d) L. M. Shkolnikova, A. A. Masyuk, G. V. Polyanchuk, E. G. Afonin, A. L. Poznyak, V. E. Zavodnik, *Koord. Khim.* **1989**, *15*, 1424.

[12] a) E. Galdecka, Z. Galdecki, P. Gawryszewska, J. Legendziewicz, *New J. Chem.* **2000**, *24*, 387–391; b) J. Legendziewicz, P. Gawryszewska, E. Galdecka, Z. Galdecki, *J. Alloys Compd.* **1998**, *275*, 356–360; c) C. Serre, N. Stock, T. Bein, G. Ferey, *Inorg. Chem.* **2004**, *43*, 3159–3163.

[13] a) R. C. Wang, Y. P. Zhang, H. L. Hu, R. R. Frausto, A. Clearfield, *Chem. Mater.* **1992**, *4*, 864–871; b) T. Glowiak, E. Huskowska, J. Legendziewicz, *Polyhedron* **1991**, *10*, 175–178.

[14] a) F. S. Richardson, *Chem. Rev.* **1982**, *82*, 541; b) W. D. Horrocks, D. R. Sudnik, *J. Am. Chem. Soc.* **1979**, *101*, 334; c) C. H. Evans, *Biochemistry of the lanthanides*, *Vol. 8*, Biochemistry of the Elements series, Plenum, New York, **1990**; d) J. Legendziewicz, *J. Appl. Spectrosc.* **1995**, *62*, 189.

[15] J.-L. Song, C. Lei, J.-G. Mao, *Inorg. Chem.* **2004**, *43*, 5630–5634.

[16] a) C. N. R. Rao, S. Natarajan, R. Vaidhyanathan, *Angew. Chem.* **2004**, *116*, 1490–1521; *Angew. Chem. Int. Ed.* **2004**, *43*, 1466–1496 (and references therein); b) H. Steinfink, G. D. Brunton, *Inorg. Chem.* **1970**, *9*, 112; c) F. Fourcade-Cavillou, J.-C. Trombe, *Solid State Sci.* **2002**, *4*, 1199–1208; d) S. Romero, A. Mosset, J. C. Trombe, *J. Solid State Chem.* **1996**, *127*, 256–266; e) I. A. Kahwa, F. R. Fronczek, V. Selbin, *Inorg. Chim. Acta* **1984**, *82*, 167.

[17] a) G. A. Hebbink, L. Grave, L. A. Woldering, D. N. Reinhoudt, F. C. J. M. van Vegel, *J. Phys. Chem.* **2003**, *A107*, 2483–2491; b) S. Faulkner, S. J. A. Pope, *J. Am. Chem. Soc.* **2003**, *125*, 10526–10527; c) S. J. A. Pope, A. M. Kenwright, V. A. Boote, S. Faulkner, *J. Chem. Soc. Dalton Trans.* **2003**, 3780–3784.

[18] W.-K. Wong, H. Liang, J. Guo, W.-Y. Wong, W.-K. Lo, K.-F. Li, K.-W. Cheah, Z. Zhou, W.-T. Wong, *Eur. J. Inorg. Chem.* **2004**, 829–836.

[19] G. M. Sheldrick, *SHELXTL*, Crystallographic Software Package, SHELXTL, Version 5.1, Bruker-AXS, Madison, WI, **1998**.

Received: August 8, 2004
Published online: January 13, 2005